Electromechanical Energy Conversion Systems (EECS),
Niroo Research Institute.
Vol. 01, Issue. 01. Winter 2021

PROVIDING A METHOD FOR IMPROVING THE STARTUP CONDITIONS OF INDUCTION MOTORS BASED ON CHANGING THE LOAD CHARACTERISTICS

E. Dehjoo[1], R. Haghmaram[1], A.Mosallnejad[*2]

[1]Department of Electrical Engineering, Imam Hussein Comprehensive University, Tehran.

[2]Department of Electrical Engineering, Shahid Beheshti University, Tehran

***Corresponding author,** Email: a_mosallanejad@sbu.ac.ir*

Abstract

In this paper, the problem of starting an induction motor is investigated and a solution is presented. The large current and considerable torque pulsation of the starting can damage the motor and other consumers connected to the feed line, and increasing the startup time will cause more heat and damage to the winding insulators. Various methods exist for startup of the induction motor, including the stator voltage control via wye-delta circuit breaker, autotransformer, and new methods such as soft starter, as well as methods for controlling the rotor's resistance, and control of V/f. However, in this research, by connecting a torsion spring between the motor shaft and the load, a new method of startup has been proposed. Therefore, due to the delay in the rotation of the load during the absorption of energy in the torsion spring it is possible to rotate loads with a torque beyond the motor starting torque, and to reduce the motor startup time as much as 77%. These cases increase the lifetime of the motor, and reduce economic costs.

Keywords: Induction Motor, Spring Starting, D-Q Transformation, Starting Current, Starting Torque, Load Model, Dynamic Modeling

1. INTRODUCTION

Motor is the most widely used motor in various industries. Among the advantages of these machines are robustness, reliability, low cost, high efficiency and good self-starting capability [1]. Direct startup of large AC motors may cause difficulties for the motor and its loads due to the voltage dips in the power supply during startup, particularly in a weak power system [2], [3]. An uncontrolled startup of motor may cause a relay cutoff in either overload or under voltage relays, resulting in startup failure [4]. Torque pulsation is often large and varies from positive to negative values. These torque transients in a motor shaft are transmitted to the load, resulting in mechanical wear in the motor bearings and the load couplings [5].

Various researches have been conducted into the starting and speed control of the induction motors. These activities include stator voltage control [6], such as traditional methods of Wye-Delta starting [7] and autotransformer [8], and new methods such as soft starters using silicon-controlled rectifiers (SCRs). These new methods are widely used in industry[9].

There are additional starting methods of controlling the rotor's resistance [10], v/f control [11], pole changing [12], and frequency changing [13]. Reducing motor starting torque or increasing load torque will increase acceleration period and starting time [14]. Therefore, it will generate more heat and damage the insulation of the windings [15].

In this research, by making changes to the load, a new model is provided for starting. This model has the ability of better starting by reducing the starting time. The paper is organized as follows: Section 2 presents the d-q transformation for induction motor, and Section 3 presents the springs starting. Section 4 describes modulation in the MATLAB/SIMULINK setting, Section 5 show simulation results, and finally Section 6 presents the conclusions of the paper.

2. D-Q TRANSFORMATION FOR INDUCTION MOTOR

Direct Quadrature (d-q) transformation is a mathematical transformation used to simplify analysis of the three-phase circuit. In the case of balanced three-phase circuits, application of d-q transformation reduces the three quantities to 2 quantities. Simplified calculations can then be conducted on these imaginary quantities before performing the inverse transformation to recover the actual three-phase ac result. The d-q transformation equations for the three-phase voltages are presented as follows [16]:

$$v_{sd} = \sqrt{\frac{2}{3}}\left(\cos\left(\theta_d v_a\right) + \cos\left(\left(\theta_d + 2\pi/3\right) v_b\right) + \cos\left(\left(\theta_d + 4\pi/3\right) v\right)\right) \quad (1)$$

$$v_{sq} = \sqrt{\frac{2}{3}}\left(\sin\left(\theta_d v_a\right) + \sin\left(\left(\theta_d + 2\pi/3\right) v_b\right) + \sin\left(\left(\theta_d + 4\pi/3\right) v\right)\right) \quad (2)$$

v_a, v_b, v_c: Three-phase voltages applied to the stator

v_{sd}, v_{sq}: Stator voltages in the direct (d) and quadratic (q) axes

θ_d: Angular position of the reference frame

For power system studies, induction machine loads and the other types of power system components are usually simulated on the system's synchronously rotating reference frame. However, for the transient studies of variable-speed drives, it is easy to simulate an induction machine and its converter on a stationary reference frame [17]. If the reference frame is considered at synchronous speed, the flux equations of the stator and rotor are as follows:

$$\varphi = \omega_b \lambda \quad (3)$$

$$\varphi_{qs} = \omega_b \int (v_{qs} + (\omega_e/\omega_b)\varphi_{ds} + (r_s/x_{ls})(\varphi_{mq} - \varphi_{qs}))dt \quad (4)$$

$$\varphi_{ds} = \omega_b \int (v_{ds} + (\omega_e/\omega_b)\varphi_{qs} + (r_s/x_{ls})(\varphi_{md} - \varphi_{ds}))dt \quad (5)$$

$$\varphi'_{qr} = \omega_b \int (v'_{qr} - (\omega_r - \omega_e/\omega_b)\varphi'_{dr} + (r'_r/x'_{lr})(\varphi_{mq} - \varphi_{qr}))dt \quad (6)$$

$$\varphi'_{dr} = \omega_b \int (v'_{dr} - (\omega_r - \omega_e/\omega_b)\varphi'_{qr} + (r'_r/x'_{lr})(\varphi_{md} - \varphi_{dr}))dt \quad (7)$$

$$X_M = \left(\frac{1}{x_m} + \frac{}{x_{ls}} + \frac{1}{x'_{lr}}\right) \quad (8)$$

$$\varphi_{mq} = X_M\left(\frac{\varphi_{qs}}{x_{ls}} + \frac{'_{qr}}{'_{lr}}\right. \quad (9)$$

$$\varphi_{md} = X_M\left.\frac{ds}{x_{ls}} + \frac{\varphi'_{dr}}{x'_{lr}}\right) \quad (10)$$

$\varphi_{ds}, \varphi_{qs}$: The stator flux on the direct (d) and quadratic (q) axes

$\varphi'_{dr}, \varphi'_{qr}$: The rotor flux referred to the stator on the direct (d) and quadratic (q) axes

r_s, x_{ls}: The resistance and leakage reactance of the stator

r'_r, x'_{lr}: The resistance and leakage reactance of the rotor referred to the stator

x_m: Magnetizing reactance

X_M: Equal reactance

ω_r: Rotor angular speed

ω_b: Synchronous angular speed

ω_e: Angular speed of the reference frame

The current equations of the stator and rotor are as follows:

$$i_{qs} = \frac{\varphi_{qs} - \varphi_{mq}}{x_{ls}} \quad (11)$$

$$i_{ds} = \frac{\varphi_{ds} - \varphi_{md}}{x_{ls}} \quad (12)$$

$$i'_{qr} = \frac{\varphi'_{qr} - \varphi_{mq}}{x'_{lr}} \quad (13)$$

$$i'_{dr} = \frac{\varphi'_{dr} - \varphi_{md}}{x'_{lr}}$$

(14) i_{ds}, i_{qs}: Stator currents in direct (d) and quadratic (q) axes

i'_{dr}, i'_{qr}: Rotor currents referred to the stator in direct (d) and quadratic (q) axes

To solve starting problems, this paper presents a new method for starting the motor by changing the load characteristics.

3. SPRING STARTING

Fig.1 presents the spring used in this research is a spiral torsion spring. Creating a torque on the spring causes the spring to be compressed around its center. Placing the spring between the load and the motor shaft can prevent the load from being applied to the motor shaft at the starting. Fig.2 shows the arrangement of the spring on the motor shaft. The spring inner head is connected to the motor shaft. Each of the two sides of the spring bearings mounted on the motor shaft. A metal cylinder is placed over the bearings, and the outer head of the spring is connected to the body of this cylinder. Since the mechanical load of the motor must be placed on this cylinder, it is defined as the secondary shaft of the motor.

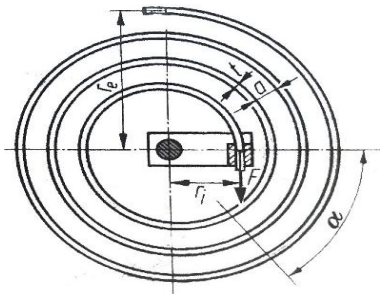

Fig.1. SPIRAL TORSION SPRING

Additionally, the mechanical load placed on the secondary shaft is defined as the secondary load, and the load received by the shaft is defined as the primary load. After starting the motor, the motor shaft starts to rotate and the spring will start to compress, since at the first moments, the outer head of the spring remains constant due to the connection to the secondary load. Inner head of the spring will start to rotate. By rotating the inner head of the spring, energy will be stored in the spring. This energy will create a force on both the inner and outer heads of the spring.

The inner and outer heads of the spring will not be able to discharge energy stored in it due to the electromagnetic torque of the motor and resistant torque of the load. Therefore, with motor shaft rotation, the energy stored in the spring and the primary load torque will gradually be increased. These conditions will be continued until the energy stored in the spring finds the force needed to overcome the secondary load. At this time, the primary and secondary loads will be equalized. Therefore, the secondary load with a little pulsation starts to rotate at a speed equal to the motor speed. By designing a suitable spring, the load rotation time can be set at a point where the motor has completed its starting mode.

Since the spring is involved in loading, motor torque equation will be changed. To investigate these changes, we first need to study the spring equations as follows [18]:

$$\alpha = \frac{\tau_{sp} 10^3 L}{EI} \tag{15}$$

Where

α: Torsion angle in rad

τ_{sp}: Springs torque in N.m

L: Length of active material in mm

I: Axial moment of inertia in mm^4

E: Modulus of elasticity in N/mm^2

The L and I for spiral torsion springs are expressed as follows:

$$I = \frac{bt^3}{12} \tag{16}$$

$$\begin{cases} L = \pi(r_e + r_i)n \\ r_e = r_i + n(t+a) \end{cases} \rightarrow \tag{17}$$

$$L = \pi(r_i + n(t+a) + r_i)n = n\pi(2r_i + nt + na)$$

where

b: Belt width of the spring in mm

t: Belt thickness of the spring in mm

r_e: Outer ring radius of the spring in mm

r_i: Inner ring radius of the spring in mm

n: Number of the spring rings

a: Distance between the rings in mm

Now τ_s is expressed in term of α as follows:

$$\tau_{sp} = \frac{EI}{L}\alpha 10^{-3} = \frac{\frac{bt^3}{12}10^{-3}}{n\pi\left(2r_i + nt + na\right)}E\alpha \quad (18)$$

$$= \frac{bt^3 10^{-3}}{12n\pi\left(2r_i + nt + na\right)}E\alpha$$

$$\tau_{sp} = R_t\alpha \rightarrow$$

$$R_t = \frac{Ebt^3 10^{-3}}{12n\pi\left(2r_i + nt + na\right)} \quad (19)$$

R_t: Spring Stiffness

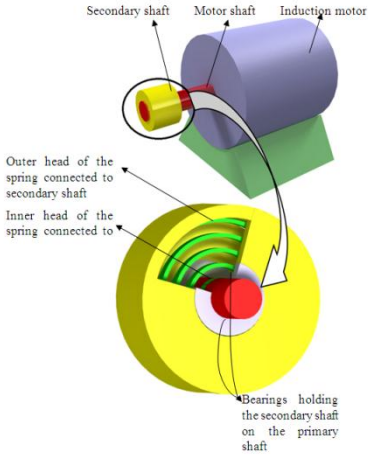

Fig. 2. HOW TO PUT THE SPRINGS ON THE SHAFT

Stress-strain diagram of each material can be drawn [19]. According to Appendix 1, the amount of stress allowed to stay in a material such as steel in the linear limit is approximately $200\times10^9\ N/m^2$. If this quantity is multiplied in the cross-section area of the spring, the force required to remove the spring from the elastic limit will be achieved

$$\text{if}\begin{cases} b = 1\times10^{-3} \\ t = 3\times10^{-3} \end{cases}$$

$$\rightarrow F = (200\times10^9)(3\times10^{-6}) \quad (20)$$

$$= 600\times10^3$$

According to Table 1, the secondary load equals 23 N.M. By applying the spring on the motor shaft, the torque arm in the worst case will be the inner ring of the spring.

$$\tau_{mec} = F r_i \rightarrow F = \frac{\tau_{mec2}}{r_i} \quad (21)$$

If r_i is equal to 9×10^{-3}, then

$$F = \frac{23}{9}\times10^3 = 2/55\times10^3.$$

Therefore, by choosing the least amount for the spring parameters, the force of the motor will not be able to overcome the force required to remove the spring from the elastic limit. Consequently, it would be possible to build the spring.

3.1. New Torque-Speed Equation

Electromagnetic torque and torque-speed equations are as follows [17]:

$$\tau_{em} = \frac{3p}{4w_b}\left(\varphi_{ds}i_{qs} - \varphi_{qs}i_{ds}\right) \quad (22)$$

$$\tau_{em} - \tau_l = J\frac{d(\omega_r)}{dt} \quad (23)$$

τ_{em}: Electromagnetic torque

p: Pole number of motor

τ_l: Torque of the secondary load

J: Moment of inertia

ω_r: Rotor angular speed

By adding the spring, the torque-speed equation will be as follows:

$$\begin{cases} \text{shaft side}: \tau_{em} - \tau_{sp} = J_r\dfrac{d\omega_r}{dt} \\ \text{Load side}: \tau_{sp} - \tau_{load} = J_{load}\dfrac{d\omega_{load}}{dt} \end{cases} \quad (24)$$

Where τ_{sp}: Torque of the primary load or spring torque.

Since the spring is not charged or discharged all over the operation period, then the rotor and springs angular position will not be equal $(\alpha \neq \theta_r)$. However, at the starting time and when the load of motor changes, the The spring torque equation is as follow.

$\tau_{damp,spring}$: Inherent torque of spring angular position of springs will be changed.

c : damping factor

θ_r: Rotor angular position

$\theta load$: Rotor angular position

Therefore, the equations of the motor simulation will be completed.

$$\begin{cases} \tau_{sp} = \tau_{spring} + \tau_{damp,spring} \\ \tau_{spring} = R_t\theta_{sp} = R_t\left(\theta_r - \theta_{load}\right) \\ = R_t(\int \omega_r dt - \int \omega_{load} dt) \\ \tau_{damp,spring} = c\dfrac{d\theta_{sp}}{dt} = \left(\dfrac{d\theta_r}{dt} - \dfrac{d\theta_{load}}{dt}\right) \\ = c\left(\omega_r \quad \omega_{load}\right) \end{cases} \quad (25)$$

4. SIMULATION INMATLAB/SIMULINK

MATLAB/SIMULINK is a system simulator that cannot simulate electrical circuits directly. Therefore, to simulate circuits, a block set an electrical is used, which incorporates libraries of electrical blocks and analysis tools to convert electrical circuits to SIMULINK diagrams [16]. The main advantage of the SIMULINK over other programming software is that the simulation model is systematically developed using basic function blocks [20]. Using Eq. (3) and Eq. (2) the three-phase voltages will be converted to voltages of direct (d) and quadratic (q) axes. Then, using Eqs (5) to (14), the block diagrams of direct (d) and quadratic (q) axes will be created. Fig. 3 shows the block diagram of the direct axis (d). Similarly, the quadratic axis (q) can be created. The simulation equations of the rotor are expressed in Eq. (24). Therefore, the simulation of the induction motor is completed. Fig. 4 presents the block diagram of the overall simulation.

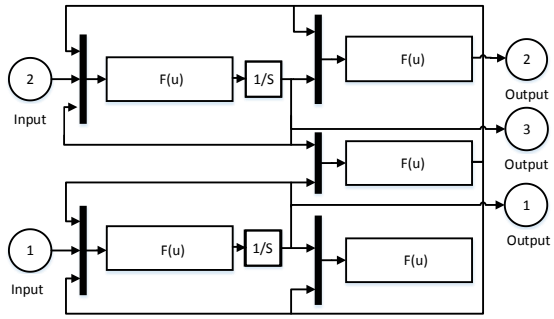

Fig. 3. BLOCK DIAGRAM OF THE DIRECT (d) AXIS

5. SIMULATION RESULTS

To validate the proposed model, parameters of reference [16] are used in the designed model. Fig. 5 shows the results of the proposed model for the electromagnetic and load torques which is similar to [16].

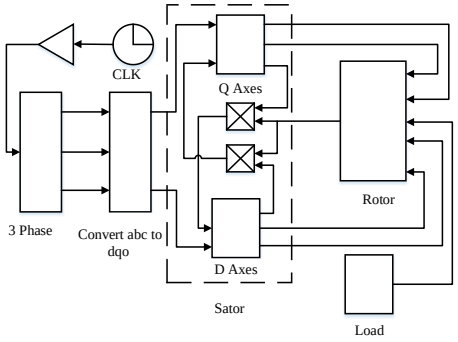

Fig. 4. BLOCK DIAGRAM OF THE INDUCTION MOTOR

Table 1 presents the parameters of the induction motor used in simulation, and simulation is performed using these values in two modes: springs mode and non-springs mode. The results of spring mode are shown with blue dashed line and those of non-spring mode is shown with red line, while the black dotted line represents the non-load results.

The starting current of the induction motor is 5 to 8 times than the steady state current. In this paper, the starting time is defined as follows: From the moment of connecting the motor to the network until the motor current drops to the steady state amount, at which moment the load torque and electromagnetic torque are equal to less than 3% accuracy. To model the spring, the starting time of motor with τ_{mec1} must be obtained.

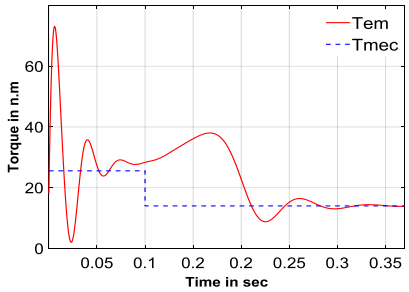

Fig. 5. ELECTROMAGNETIC AND LOAD TORQUE OF [16]

Given the stator current curve in constant load shown in Fig. 7 and electromagnetic torque in Fig. 9, the starting time is obtained 1.38 sec. Now, the spring angular deflection according to Fig. 5 is equal to 43.05 rad. Therefore, by numbering in Eq. (19), the spring stiffness will be obtained as follows:

$$\tau_s = R_t\alpha \rightarrow 13 = R_t 43.05 \rightarrow R_t = 0.3\frac{\text{N.m}}{\text{rad}} \quad (26)$$

As Fig. 7 and Fig. 9 shows, starting time in the non-springs mode is equal to 1.28 sec, while in spring mode, it decreases to 0.29 sec. Therefore, the starting time has been reduced by 77 percent, which will

cause to increase the lifetime of the stator winding.

Table. 1. The Parameters Of The Induction Motor

Parameter	Symbol	Value
Number of poles	p	4
Frequency	f	60
Maximum voltage	V_m	375.58 V
Stator resistance	r_s	1.77 Ω
Leakage reactance of the stator	X_{ls}	5.25 Ω
Rotor resistance referred to the stator	r'_r	1.34 Ω
Leakage reactance of the rotor referred to the stator	X'_{lr}	4.57 Ω
Magnetizing reactance	X_m	139 Ω
Moment of inertia	J	0.025 kg/m^2
First value of the secondary load torque	$\tau_{mec\,1}$	13 N.m
Second value of the secondary load torque	$\tau_{mec\,2}$	23 N.m

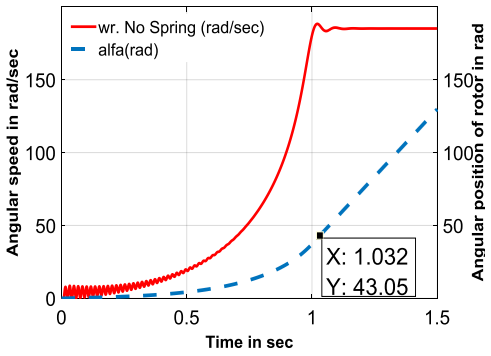

Fig. 6. Rotor Angular Speed And Rotor Angular Position In Non-Spring Mode

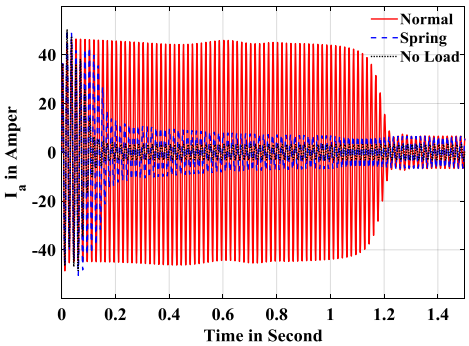

Fig. 7. Stator Phase Current I_A With 13 N.m Load Torque

As Fig. 8 shows, the amplitude and frequency of the rotor starting current with springs behind faster the starting condition than the non-spring mode. Consequently, the lifetime of rotor winding will increase with spring.

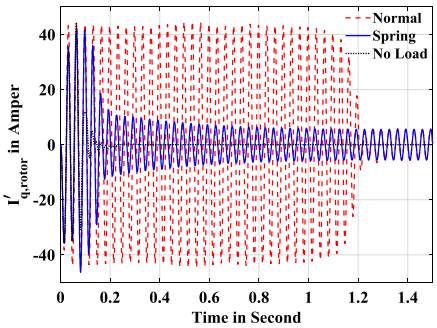

Fig.8. Rotor Phase Current Referred To The Stator In The Direct (D) Axis With 13 N.m Load

Fig. 9 presents the electromagnetic torque of the motor. In the spring starting mode, the number of electromagnetic and speed pulsation has decreased. Therefore, failure of mechanical parts such as motor bearings reduces in this mode.

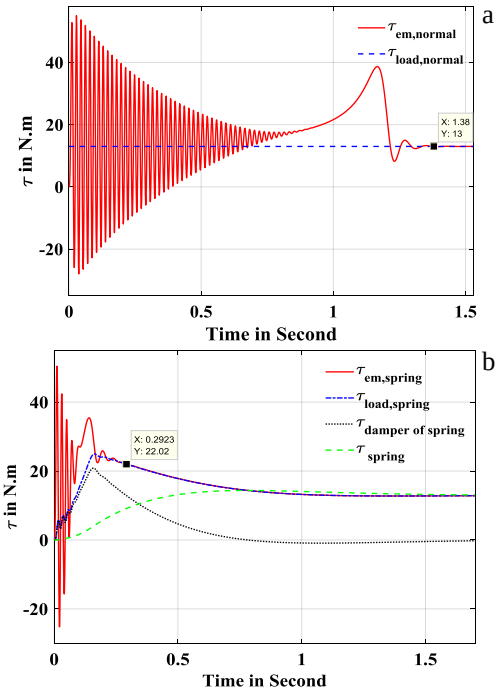

Fig. 9. Electromagnetic Torque: (a) Without Springs (b), With Springs

The value of $\tau_{mec\,1}$ was less than the starting torque of motor. Now, the secondary load torque is changed to $\tau_{mec\,2}$, and this value is higher than the starting torque of the motor. Again, the simulation is performed in two different modes, with spring and without it. In

non-spring mode, since the primary torque load is higher than the starting torque, the motor could not start. In the spring mode, although the secondary torque is higher than starting torque, the primary torque is lower than the starting torque. Therefore, the induction motor can be started. This result is confirmed in Figs. 10 and 11. Figs. 10 and 11 show the stator current and the electromagnetic torque curves, respectively.

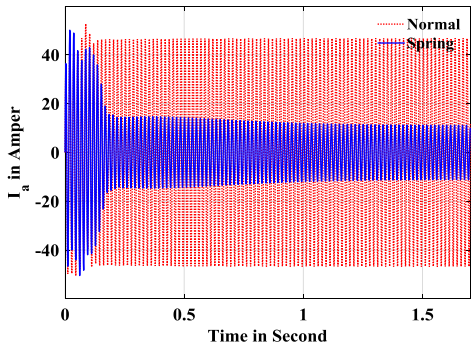

Fig. 10. STATOR PHASE CURRENT I_A WITH 23 N.m LOAD TORQUE

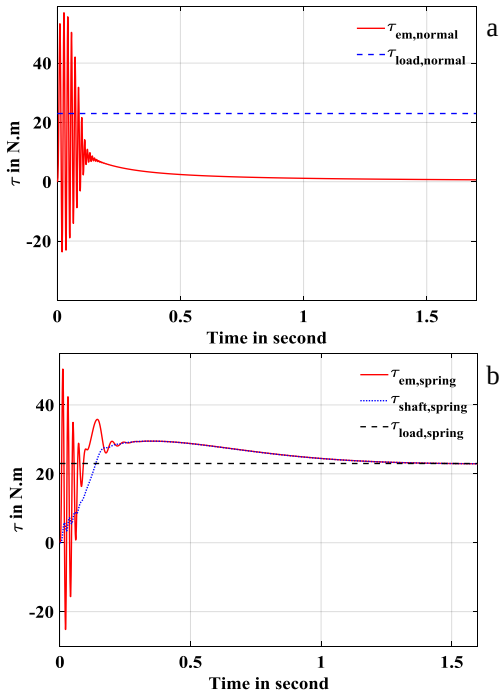

Fig. 11. ELECTROMAGNETIC TORQUE: (a) WITHOUT SPRING (b), WITH SPRING

6. CONCLUSION

In this paper, to have a new idea for starting induction motor, the spiral torsion spring is applied on the rotor shaft. Using the simulation of MATLAB/SIMULINK, the induction motor in constant load is simulated in two modes with spring and without it. The performance of motor parameters was investigated. In a spring mode compared to non-spring mode, the starting time is reduced by 77 percent. Therefore, time of voltage drops due to starting, failure of mechanical parts such as motor bearings, rotor damage and stator winding was reduced. Consequently, the lifetime of motor would increase. In the spring mode, it is possible to start motor in loads with a torque greater than the starting torque and even a load with the maximum torque of the motor. Thus, the size of motor can be reduced to the constant load. As a result, the economic costs were reduced. However, in the spring mode, the motor is not rotated in two directions. Furthermore, the investigation of motor loading in different loads by the spring starting is introduced as a future study plan.

7. REFERENCES

[1] M. Salahat, O. Barbarawe, M. A. Zalata, and S. J. E. Asad, 2011. "Modular Approach for Investigation of the Dynamic Behavior of Three-Phase Induction Machine at Load Variation," ***Engineering***, vol. 3(5), p: 525-531.

[2] G. Zenginobuz, I. Cadirci, M. Ermis, and C. Barlak,. 2004. "Performance optimization of induction motors during voltage-controlled soft starting," ***IEEE Transactions on Energy Conversion***, vol. 19(2), p: 278-288.

[3] J. Nevelsteen and H. Aragon, 1968. "Starting of large motors-methods and economics," ***IEEE Transactions on Industry Applications***, vol. 25(6), p: 1012-1018, Nov.-Des. 1989.

[4] G. Zenginobuz, I. Cadirci, M. Ermis, and C. Barlak, 2001. "Soft starting of large induction motors at constant current with minimized starting torque pulsations," ***IEEE Transactions on Industry Applications***, vol. 37(5), p: 1334-1347.

[5] M. G. Solveson, B. Mirafzal, and N. A. Demerdash, 2006. "Soft-started induction motor modeling and heating issues for different starting profiles using a flux linkage ABC frame of reference," ***IEEE Transactions on Industry Applications***, vol. 42(4), p: 973-982.

[6] D. A. Paice, 1968."Induction motor speed control by stator voltage control," ***IEEE Transactions on power Apparatus systems***, vol. PAS-87(2), p: 585-590.

[7] R. F. McElveen and M. K. Toney,. 2001. "Starting high-inertia loads," ***IEEE Transactions on Industry Applications***, vol. 37(1), p: 137-144.

[8] H. Goh, M. Looi, and B. Kok,. 2009. "Comparison between direct-on-line, star-delta and auto-transformer induction motor starting method in terms of power quality," ***in Proc. IMECS, Hong Kong***. vol. 2, p: 1558-1563.

[9] C.-C. Yeh and N. A. Demerdash,2009. "Fault-tolerant soft starter control of induction motors with reduced transient torque pulsations," ***IEEE Transactions on Energy Conversion***, vol. 24(4), p: 848-859, .

[10] R. Hamouda, A. Alolah, M. Badr, and M. Abdel-Halim,. 1999. "A comparative study on the starting methods of three phase wound-rotor induction motors. I," ***IEEE Transactions on Energy Conversion***, vol. 14(4), p: 918-922.

[11] A. Munoz-Garcia, T. A. Lipo, and D. W. Novotny, 1998. "A new induction motor V/f control method capable of high-performance regulation at low speeds," ***IEEE transactions on Industry Applications***, vol. 34(4), p: 813-882.

[12] M. Osama and T. A. Lipo, .1997. "Modeling and analysis of a wide-speed-range induction motor drive based on electronic pole changing," ***IEEE Transactions on Industry Applications***, vol. 33(5), p: 1177-1184,.

[13] A. Nabae, K. Otsuka, H. Uchino, and R. Kurosawa, 1980. "An approach to flux control of induction motors operated with variable-frequency power supply," ***IEEE transactions on Industry Applications***,Vol. 3, P:. 342-350, May 1980.

[14] M. Toman, R. Cipin, M. Mach, and P. Vorel, "Application of acceleration method for evaluation of induction motor torque-speed characteristics," in EEEIC/I&CPS Europe Milan, 2017, p: 1-4.

[15] P. C. Sen, "Induction (asynhronous) machines," in Principles of Electric Machines and Power Electronics,3th ed. Hoboken: Wiley, 2013, p: 259-267.

[16] S. Shah, A. Rashid, and M. Bhatti, 2012. "Direct quadrate (dq) modeling of 3-phase induction motor using matlab/simulink," ***Canadian Journal on Electrical Electronics Engineering***, vol. 3(5), p: 237-243.

[17] S. K. Jain, F. Sharma, and M. K. Baliwal,. 2014. "Modeling and Simulation of an Induction Motor," ***International Journal of Engineering Research Development***, vol. 10(4), p: 57-61.

[18] K. H. Decker, K. Kabus, and F. Rieg, "Federn. 2011." in Maschinenelemente Funktion, Gestaltung und Berechnung,Berlin, ***DEU: Hanser***, p: 309-321.

[19] J. E. Shigley, 2011. "Materials," ***in Shigley's mechanical engineering design,10th ed. New York: McGraw-Hill***, p: 42-51.

[20] H. Arabaci and O. Bilgin, 2012."Squirrel Cage of Induction Motors Simulation via Simulink," ***International Journal of Modeling Optimization***, vol. 2(3), p: 324-327.

Appendix

Fig. A1 shows the stress-strain diagram for ductile materials obtained from the standard tensile test. The stress and strain equations are defined as follows:

$$\epsilon = \frac{\delta}{l} \text{ and } \sigma = \frac{P}{A_0} \qquad (A1)$$

ϵ: Strain, σ: Stress, P: Load applied to the material A_0: Cross section of the material, δ: Change of the length

Point *pl* in Fig. A1 is called the proportional limit. This is the point at which the curve first begins to deviate from a straight line. No permanent set will be observable in the specimen if the load is removed at this point. In the linear range, the uniaxial stress-strain relation is presented by Hooke's law as:

$$\sigma = E\epsilon \qquad (A2)$$ E: Modulus of elasticity

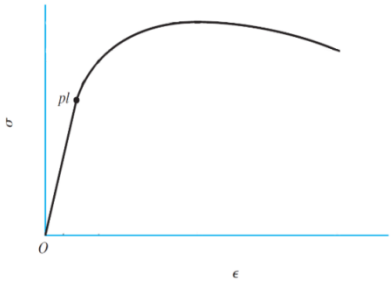

Fig. A1. STRESS-STRAIN DIAGRAM

The steel has a modulus of elasticity of approximately 207 GPa regardless of heat treatment, carbon content, or alloying. Stainless steel is approximately 190 GPa.